Examples of Infrasonic Propagation over Topography

David Green, Blacknest
July 26, 2016

1 Background

Propagation of infrasound over topography is rarely considered when undertaking propagation modelling for studies of interest to the Comprehensive Nuclear-Test-Ban Treaty monitoring network. Although topography has been considered on near-regional scales (e.g., McKenna et al., 2012; Kim and Lees, 2014), it has only been added in a very ad-hoc manner to a few longer range propagation studies (e.g., Figure 8 of Arrowsmith and ReVelle, 2007). In addition, simple cases (such as might be developed in a scaled laboratory setting) have not been considered. Codor Khodr has started a PhD project in the Faculty of Engineering at the University of Bristol to address this knowledge gap. He has begun (since November 2015) to develop models (PE, FEM) that will enable us to better understand the magnitude of topographic effects.

In order to tailor his modelling work, Codor needs to understand what type of topographic interactions are of interest. In these 'working notes' I provide some ideas and suggestions. I anticipate that I will update this as I collect more examples.

2 Scalelengths

There are two scalelengths that I am interested in, for two different purposes.

1. **Along-ground infrasonic propagation** within the troposphere (often called the direct wave). This is often the wave we are interested in if undertaking a field campaign at explosive trials and/or a volcano: we position our sensors close ($<$10 km) to the source. In these cases the interaction of the wave with the ground surface and the winds of the lower troposphere influence the signals one observes. Complex modelling in 3D can help (e.g., Kim and Lees, 2014), but simple cases that help us understand the interaction of infrasound with topography have yet to be undertaken.

2. **Interaction with topography along long-range propagation paths**. The majority of long-range infrasound signals ($>$500 km path length) will have propagated from the source up into the middle atmosphere, returned to the ground surface, and then been reflected back into the atmosphere from the ground surface (see, for example, the PE modelling results in Figure 4 of Assink et al., 2014). Current modelling practice is to consider the ground surface as a perfectly reflecting flat plate: what effect does topography have?

3 Possible Case Studies: Along-ground infrasound propagation

3.1 Erebus Volcano, Antarctica

Johnson et al. (2012) presented work from Villarica, Chile, that showed that the wavefield must interact with topography as it propagates downslope from the volcano to the receiver. However, the modelling undertaken in this paper was restricted to the high-frequency limit (ray-theory) and therefore only qualitative statements could be made about diffraction.

It would be interesting to understand the quantiative effects of different slopes (and topographic barriers) on the propagation of infrasound from volcanoes, as almost always the near-field sensors are at altitudes below the summit. One possible area of study would be Mount Erebus in Antarctica. See, for example, Dabrowa et al. (2014) for a recent study of infrasound at a range of approximately 25 km from the summit. However, getting hold of a Digital Elevation Model may prove difficult.

3.2 Sayarim, 2011: Israel

The Sayarim Infrasound Calibration shots provided a wealth of infrasound data from explosions, some of it at local to near-regional ranges (e.g., Fee et al., 2013; Bonner et al., 2013a). Figure 14 of Bonner et al. (2013b) exhibits some amplitude variation that the authors suggest may be due to topographic influence (both enhancement on top of local hills, and topographic shadowing at greater distance). Although I do not have the data at present, I am currently working closely with the authors of this paper so it should be possible to get this data.

However, for this case we'd need to have a modelling capability that incorporated both topographic and wind effects (as both are important in the observed signals).

3.3 Ascension Wind Turbine Noise

When I started at Blacknest, I spent a lot of time looking at data in order to try and work out what different noise sources might be. One major contributor at certain stations are wind farms. This is especially true at Ascension Island where there is an infrasound station, I50GB, centred at 7.937740S, 14.375170W (easy to spot on Google Earth). At the time I was looking at signals there was only one wind farm on the island (close to the runway at 7.961285S, 14.386794W). Signals from this source were easy to spot as harmonic power spikes within the power spectral density plots of the individual stations. Interestingly, there appeared to be differences between the power observed across the different elements of the array. One suggested cause of this was variable topographic blockage between the source and the eight elements of the array: this has never been tested.

Data released from the Shuttle Radar Topography Mission (http://www2.jpl.nasa.gov/srtm/) provides us with a digitial elevation dataset with approximately 90 m horizontal resolution of the area, allowing topography maps and profiles to be generated (Figures 1 and 2). This shows that there are significant differences in topographic profile between the source ('wind farm') and the receivers.

This may be a nice example to start looking at for a number of reasons:

1. We have access to all the infrasound data
2. Wind turbine noise is largely harmonic (due to the blade-pass frequency). Therefore we can isolate the effects at single frequencies, rather than an integral over a frequency band as must be done for broadband signals.
3. The topography is certainly not 2D. There will likely be appreciable 3D effects. Because the significant topography is generated by mainly ancient volcanic vents their structure is relatively simple for real-world examples (i.e., truncated cones).

4 Possible Case Studies: Long-range "ground bounce" interactions

I will attend to this section at a later date.

References

Arrowsmith, S. J. and ReVelle, D. O. Infrasound Monitoring of Local, Regional and Global Events. In *Proceedings of the 29th Monitoring Research Review: Ground-Based Nuclear Explosion Monitoring Technologies*, pages 815–824, Denver, Colorado, 2007.

Assink, J. D., Waxler, R., Smets, P., and Evers, L. G. Bidirectional infrasonic ducts associated with sudden stratospheric warming events. *J. Geophys. Res. Atmos.*, 119(3), 1140–1153, 2014.

Bonner, J., Waxler, R., Gitterman, Y., and Hofstetter, R. Seismo-acoustic energy partitioning at near-source and local distances from the 2011 Sayarim explosions in the Negev Desert, Israel. *Bull. Seism. Soc. Am.*, 103(2A), 741–758, 2013a.

Bonner, J. L., Russell, D. R., and Reinke, R. . Modeling surface waves from aboveground and underground explosions in alluvium and limestone. *Bull. Seism. Soc. Am.*, 103(6), 2953–2970, 2013b.

Dabrowa, A. L., Green, D. N., Johnson, J. B., Phillips, J. C., and Rust, A. C. Comparing near-regional and local measurements of infrasound from Mount Erebus, Antarctica: Implications for monitoring. *J. Volcanol. Geotherm. Res.*, 288, 46–61, 2014.

Fee, D., Waxler, R., Assink, J., Gitterman, Y., Given, J., Coyne, J., Mialle, P., Garces, M., Drob, D., Kleinert, D., Hofstetter, R., and Grenard, P. Overview of the 2009 and 2011 sayarim infrasound calibration experiments. *J. Geophys. Res.*, 118(12), 6122–6143, 2013.

Johnson, J. B., Anderson, J., Marcillo, O., and Arrowsmith, S. Probing local wind and temperature structure using infrasound from Volcan Villarrica (Chile). *J. Geophys. Res. Atmos.*, 117(D17), 2012.

Kim, K. and Lees, J. M. Local volcano infrasound and source localization investigated by 3d simulation. *Seism. Res. Lett.*, 85(6), 1177–1186, 2014.

McKenna, M. H., Gibson, R. G., Walker, B. E., McKenna, J., Winslow, N. W., and Kofford, A. S. Topographic effects on infrasound propagation. *J. Acoust. Soc. Am.*, 131(1), 35–46, 2012.

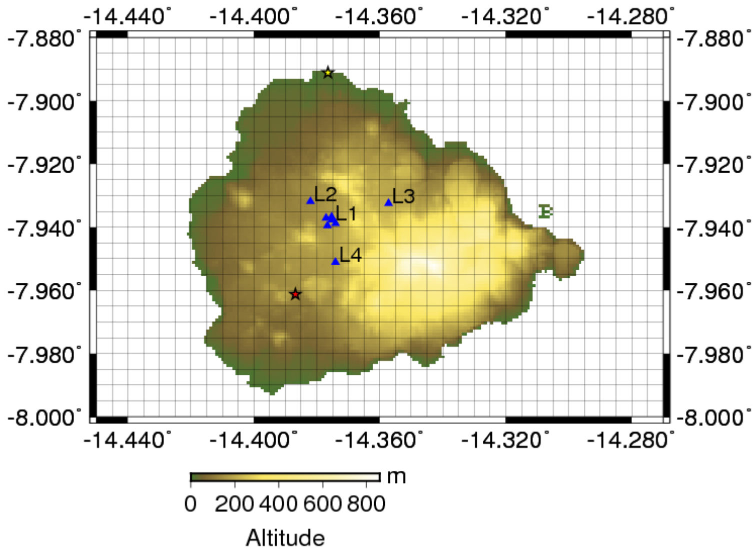

Figure 1: A map of Ascension Island, with the location of the IMS infrasound receivers of array I50GB given as blue triangles. The Ascension Island Wind Turbines are given as a red star, the recently installed (2010) BBC Wind Turbines are given as a yellow star. Labels 'L1' to 'L4' identify the four infrasound sensors connected to the large wind noise reduction systems. Along ground profiles between the Ascension Island Wind Turbines and these sensors are given in Figure 2.

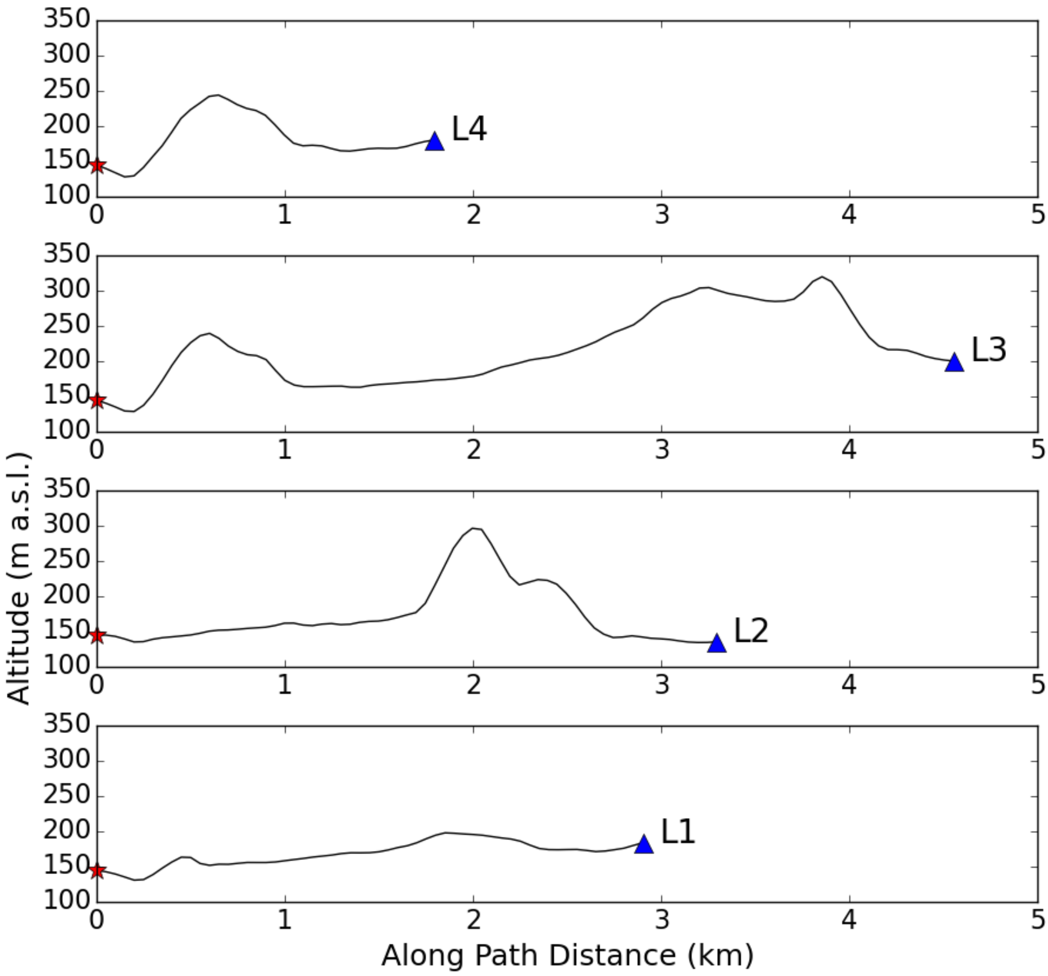

Figure 2: Along ground profiles between the Ascension Island Wind Turbines (red star) and four elements of the I50GB infrasound array (see Figure 1). Note that, although there is significant vertical exaggeration, the x- and y- scales of the four plots are identical, for ease of comparison.